

Tough reinforced open porous polymer foams via concentrated emulsion templating

Angelika Menner^a, Kristina Haibach^a, Ronald Powell^b, Alexander Bismarck^{a,*}

^a Department of Chemical Engineering, Polymer and Composite Engineering (PaCE) Group, Imperial College London, South Kensington Campus, London SW7 2AZ, UK

^b Halliburton Energy Services, 2600 South 2nd Street, P.O. Box 1431, Duncan, OK 73536-0470, USA

Received 6 May 2006; received in revised form 30 August 2006; accepted 1 September 2006

Available online 26 September 2006

Abstract

Low-density but very resilient and robust polymer foams possessing an interconnected open porous network have been synthesised by the polymerisation of the continuous phase of concentrated or high internal phase emulsions containing polyethylene glycol dimethacrylate (PEGDMA) as main crosslinker. The synthesised polymer foams did not display the undesirable properties, such as brittleness and chalkiness, which are commonly observed for highly crosslinked porous polymer monoliths synthesised by the polymerisation of high internal phase emulsions. An effective way to improve the mechanical performance of open porous polymer foams is to raise the apparent foam density. Therefore, the continuous phase of the emulsions was increased up to 40 vol.%. The mechanical properties can be further increased by the incorporation of silica particles into the polymer. Methacryloxypropyltrimethoxysilane was added to the continuous phase to ensure that the silica particles were covalently bonded into the inorganic polymer network formed by the hydrolytic condensation of the silane groups. The addition of reinforcement increased the mechanical properties. The Young's modulus and the crush strength of the polymer foams increased by up to 360% and by up to 300%, respectively, in comparison to non-reinforced samples.

© 2006 Elsevier Ltd. All rights reserved.

Keywords: Porous polymers; Composites; Emulsion template

1. Introduction

In recent years highly porous polymer foams with an interconnected pore network structure obtained from high internal phase emulsion (HIPE) templates have gained increasing interest because of their unique properties such as high porosity and high degree of pore interconnectivity. HIPEs are commonly defined as emulsions where the internal phase occupies at least 74% of the volume. The lower limit of the internal phase corresponds to the maximum packaging fraction of monodisperse spheres [1–6]. However, Lissant [1] defined emulsions having an internal phase volume fraction greater than 70% as HIPEs. The polymerisation of the continuous

organic phase leads to polymer monoliths, so called polyHIPEs, with a very high degree of porosity possessing an interconnected pore network. The spherical cavities in the polymer foams are referred to as 'pores' (Fig. 1). The pore size (Fig. 1) is defined by the droplet diameter in the emulsion template and ranges for polyHIPEs typically from 5 μm to about 100 μm . Individual pores are connected via pore throats (Fig. 1), which form during polymerisation in the area of contact points of neighbouring droplets. Their formation is a complex process and is believed to depend on many parameters, such as the volume fraction of the internal phase, the concentration of the surfactant, the droplet size, the tendency for Ostwald ripening and the nature of the polymer forming throughout the polymerisation [7–9]. Although polyHIPEs were first described in early 1970s by Lissant and Mayhan [10] and are the subject of an ever increasing number of publications and patents [11–16], they have not yet found any major

* Corresponding author. Tel.: +44 20 75 94 55 78.

E-mail address: a.bismarck@imperial.ac.uk (A. Bismarck).

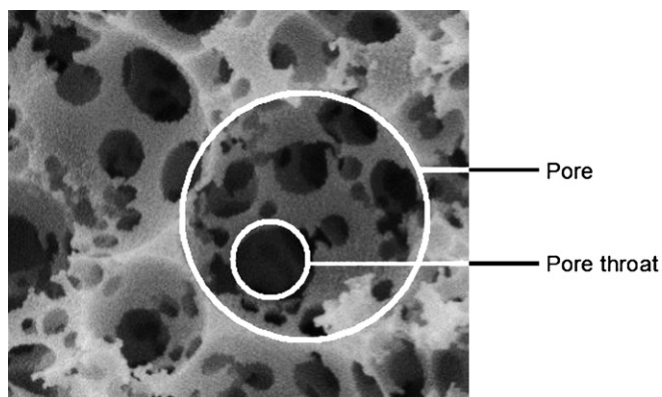


Fig. 1. Definition of pore and pore throat.

industrial applications because of their undesirable properties, such as their brittleness and chalkiness. Nevertheless, such highly porous polymer foams are explored for a number of possible applications, such as ion exchange modules [17], monolithic polymer supports for catalysis applications [18]. They are even considered for tissue engineering applications [19–21].

The first and most investigated groups of polyHIPEs are copolymers made of styrene and divinylbenzene (DVB) representing the organic phase of the emulsion [12,13–22]. More recently polyHIPEs were synthesised using other monomers, such as 4-vinylbenzyl chloride [23] and 4-nitrophenyl acrylate [18]. The chalkiness and brittleness observed for polyHIPEs based on styrene and DVB can be reduced by the use of 2-ethylhexyl acrylate (EHA) as comonomer. However, the glass transition temperature of these polyHIPEs decreases with increasing EHA content. PolyHIPEs containing more than 45 wt.% EHA are elastomers, which possess glass transition temperatures (T_g) below 25 °C. Such porous polymer monoliths are characterised by low Young's moduli and crush strengths [3–5,24]. Tai et al. [25] have synthesised polyHIPEs consisting of an inorganic polysilsesquioxane network combined with an organic polystyrene network to enhance the thermal stability of the foams. They successfully copolymerised methacryloxypropyltrimethoxysilane (MPS) with styrene and divinylbenzene. The hydrolytic condensation of the trimethoxysilyl group forms an inorganic polysilsesquioxane network within the organic polymer network. The hydrolytic condensation reaction of silane derivatives is also used for the synthesis of purely inorganic hierarchical porous monoliths [26].

The aim of this present study is to improve the mechanical properties and to reduce the chalkiness of highly porous polymer foams significantly without affecting an interconnected pore network structure. In order to achieve our objectives, we raised the continuous phase volume, found a better suited crosslinker and added particles as reinforcement. We used concentrated emulsions, or as defined by Lissant [1] medium internal phase emulsions (MIPEs), which are emulsions with an internal phase volume ranging from 30 to 70%, as templates for the synthesis of porous media, which we call

polyFoams rather than polyMIPEs. The cellular structure of the samples was studied using scanning electron microscopy (SEM). The density, porosity, Young's modulus and the thermal behaviour were characterised and compared with the properties obtained from polyHIPE and polyFoams without any reinforcement.

2. Experimental section

2.1. Materials

Styrene, polyethylene glycol dimethacrylate (PEGDMA) having a molecular weight of 330 g/mol, methacryloxypropyltrimethoxysilane (MPS), α,α' -azoisobutyronitrile (AIBN), $\text{CaCl}_2 \cdot 2\text{H}_2\text{O}$ were purchased from Sigma Aldrich (Gillingham, UK). The silica particles (main average diameter of 200 nm) were kindly supplied by Rave Produkte und Dienstleistungen (Koblenz, Germany) and the nonionic surfactant Hypermer B246sf by UNIQEMA (Wirral, UK). All chemicals were used as received.

2.2. Emulsion preparation

HIPE 1 (internal phase volume of 80%) and the concentrated MIPEs 2–6 (internal phase volume of 60%) were prepared in a reaction vessel and stirred by a glass paddle rod connected to an overhead stirrer. During the HIPE preparation the stirring rate of 400 rpm was kept constant. The liquid phase of the continuous phase of every emulsion contained 80 vol.% monomers, 20 vol.% of the surfactant Hypermer B246sf and 1 mol% AIBN as initiator. Furthermore, the continuous phase contained between 0 wt.% and 30 wt.% SiO_2 with respect to the monomers. The organic phase level of the emulsion corresponds to the total volume of the liquid components.

The continuous phase was stirred until all components were dissolved and a homogeneous suspension was achieved. After 5 min, the aqueous phase containing 2 mol/l $\text{CaCl}_2 \cdot 2\text{H}_2\text{O}$ as electrolyte to suppress Ostwald ripening was slowly added to the continuous phase, whilst the stirring rate remained constant. Once all of the aqueous phase had been added, the stirring rate was increased to 1000 rpm for a further 20 min to obtain a homogeneous but highly viscous emulsion. The composition of the emulsions is shown in Table 1.

2.3. Polymer foam preparation

The concentrated MIPEs and HIPE were transferred into flacon tubes, sealed and polymerised at 70 °C for 24 h in an oven. The polymer foams were taken out of the tubes and extracted in a Soxhlet apparatus for 72 h firstly with distilled water followed by methanol to remove any impurities. To ensure that all moisture had been evaporated, the polymer foams were dried in a vacuum oven at 70 °C until a constant weight was reached.

Table 1
Composition of the emulsion templates

Sample	Organic phase ^a [vol.%]	Organic phase composition: PEGDMA/S/MPS ^b [vol.%]/[vol.%]/[vol.%]	SiO ₂ content [wt.%] ^c
1	20	40/40/0	0
2	40	40/40/0	0
3	40	40/25/15	0
4	40	40/25/15	10
5	40	40/25/15	20
6	40	40/25/15	30

^a Volume of the organic phase relative to the total volume of the emulsion.

^b Content of PEGDMA, styrene (S) and MPS relative to the organic phase volume.

^c wt% filler relative to the monomers.

2.4. Characterisation of the polymer foams

2.4.1. Microscopy/cell structure

To determine the internal structure, i.e. the pore and pore throat size of the synthesised polymer foams, images of fractured surfaces were taken using scanning electron microscopy (Jeol JSM 5610 LV, Jeol Ltd., Welwyn Garden City, UK). Therefore, approximately 1 cm³ of each sample was fixed to a sample holder using a carbon black sticker. The sample was then placed inside an Emitech 550 (Emitech Ltd., Ashford, UK), where it was gold sputtered in an argon atmosphere to achieve the necessary conductivity.

2.4.2. Determination of the density and porosity

Density measurements were taken using a Helium Pycnometer (AccuPyc 1330, Micrometrics Ltd., Dunstable, UK). Therefore, the samples are weighted initially and then placed into measuring chamber of known volume of the pycnometer. The pressure will rise above the atmospheric value. The Helium is then expanded through a valve and its volume is measured. As a result, the pressure in the cell will fall to an intermediate value. The polymer matrix density ρ_m can then be calculated using the following equation:

$$\rho_m = \frac{m_s}{V_C - \frac{V_{EXP}}{\left(\frac{p_{1G}}{p_{2G}} - 1\right)}} \quad [\text{g/cm}^3] \quad (1)$$

where m_s is the sample mass, V_C the cell volume, V_{EXP} the expanded volume, p_{1G} the cell elevated pressure and p_{2G} the cell intermediate pressure. The envelope or foam density and porosity of the sample were measured using an envelope density analyzer (GeoPyc 1360, Micrometrics Ltd., Dunstable, UK). This instrument determines the external (envelope) volume of the sample so that the internal pores are considered to be part of the sample (V_{P+M}). By subtracting the sample material volume, determined using the helium pycnometer (V_M) (which does not consider the pores as part of the sample volume), the total pore volume (V_P) can be determined. This can be summarised by the following Eq. (2):

$$V_P = V_{P+M} - V_M \quad [\text{cm}^{-3}] \quad (2)$$

The GeoPyc determines the external sample volume by measuring how far a plunger can be driven by a stepping motor into a cylinder containing a mixture of graphite powder and the sample. When the sample mass is divided by envelope volume the envelope or foam density (ρ_f) is obtained (Eq. (3)). The porosity (P) is found using Eq. (4):

$$\rho_f = \frac{m_s}{V_{P+M}} \quad [\text{g/cm}^3] \quad (3)$$

$$P = \left(1 - \frac{\rho_f}{\rho_m}\right) \times 100 \quad [\%] \quad (4)$$

2.4.3. Thermal analysis

The thermal behaviour of each sample was determined using a differential scanning calorimeter (DSC) (Pyris 1, Perkin Elmer, Boston, USA). Approximately 5 mg of each polymer foam were investigated in a temperature range from 20 to 200 °C at a heat rate of 10 °C/min. The heat flow was measured. Two heating and cooling curves were recorded.

2.4.4. Elastic modulus

A Lloyds Universal Testing Machine (Lloyds EZ50, Lloyds Instruments Ltd., Fareham, UK) equipped with a 50 kN load cell was used to measure mechanical properties in compression. The compression tests were carried out according to industrial standard BS ISO 844. The foam samples were loaded at a rate of 1 mm/min. Five samples of 25 mm in diameter and 10 mm in height were tested for each polymer foam. The samples were loaded until a displacement of half the height of the examined sample was reached. The Young's modulus was determined from the initial linear slope of the stress–strain plot. We defined the crush strength as the maximum strength at the end of the initial linear elastic region. In order to obtain the specific Young's moduli and specific crush strengths, the stress values were normalised by the individual foam densities.

3. Results and discussion

The continuous phase of HIPE 1 made up 20 vol.% whilst the continuous phase of the MIPEs 2–6 occupied 40 vol.% of the emulsion volume. HIPE 1 as well as the MIPEs 2–6 were stabilised by the nonionic, polymeric surfactant Hypermer B246sf, which is a block copolymer of a polyhydroxy fatty acid and polyethylene glycol with a hydrophilic–lipophilic balance (HLB value) of 6. Each emulsion contained PEGDMA with an average molecular weight of 330 g/mol as a crosslinker, which led to a much reduced brittleness and chalkiness of the resulting polymer foams when compared to traditional polyHIPEs containing solely DVB as crosslinker. Nevertheless, the high degree of crosslinking of the polymer resulted in the absence of a glass transition in the temperature region

Table 2
Properties of polymer foams

Sample	Pore size [μm]	Pore throat size [μm]	Matrix density ρ_m [g/cm^3]	Foam density ρ_m [g/cm^3]	Porosity P [%]
1	10 \pm 3	1 \pm 1	1.373 \pm 0.006	0.312 \pm 0.003	77 \pm 1
2	6 \pm 4	1 \pm 1	1.265 \pm 0.004	0.360 \pm 0.005	71 \pm 1
3	5 \pm 4	1 \pm 1	1.196 \pm 0.002	0.405 \pm 0.012	66 \pm 2
4	100 \pm 20	Porous microstructure	1.221 \pm 0.004	0.389 \pm 0.005	68 \pm 2
5	100 \pm 20		1.271 \pm 0.002	0.401 \pm 0.080	68 \pm 2
6	50 \pm 10		1.270 \pm 0.010	0.473 \pm 0.020	63 \pm 2

of 20–200 °C. In addition to the monomers styrene and PEGDMA the MIPEs 3–6 contained also MPS. The hydrolytic condensation of the MPS formed an inorganic network, which was chemically bound to the organic component of the network, which was formed by free radical polymerisation. The hydrolytic reaction of the silane groups made it possible to integrate the silica particles into the walls of the polyFoams 4–6. PolyFoam 3 had a similar composition as polyFoams 4–6 except it did not contain silica fillers. It was synthesised as a reference sample to underline the effect of reinforcement on foam properties. Tables 2 and 3 summarise the properties of the prepared polymer foams.

The polymerisation of HIPE 1 with an organic phase content of 20 vol.% consisting of PEGDMA and styrene led to a non-chalky, flexible and porous material. The SEM-micrographs of 1 (Fig. 2a and b) show the typical open porous network structure for polyHIPEs. The pore diameters ranged from 7 μm to 13 μm . The pores were interconnected via pore throats of about 1 μm in diameter. PolyHIPE 1 had a matrix density of 1.373 g/cm^3 , a foam density of 0.312 g/cm^3 and a porosity of 77%.

HIPE 1 was highly viscous, which made it difficult to transfer the emulsion into the flacon tube without creating any air bubbles in the emulsion. It is known that the viscosity of HIPEs and MIPEs, respectively, decreases with increasing organic phase or decreasing internal phase levels [27]. We have also shown that less concentrated emulsions with internal phase volumes up to 60 vol.% if stabilised by a suitable surfactant can act as template for the synthesis of highly porous polymer foams with a high degree of pore interconnectivity [28–30]. In order to improve the handling of the emulsion template and to increase the foam density we increased the organic phase in MIPE 2 to 40 vol.%. MIPE 2 has only 60 vol.% aqueous internal phase but nevertheless the resulting

polyFoam 2 (Fig. 3a and b) possessed a highly interconnected pore network structure. The pore diameter varied between 3 μm and 10 μm and the pore throat size ranged from 1 μm to 2 μm . Due to the high organic phase level of 40 vol.% the foam density increased to 0.360 g/cm^3 and the porosity decreased to 71% in comparison to polyHIPE 1.

MIPEs 3–6 all contained 40 vol.% continuous organic phases. The polymerisable organic phase consisted of PEGDMA, styrene and MPS. MIPE 3 was seen to be very viscous, once polymerised it resulted in polyFoam 3 with an inhomogeneous pore network structure (Fig. 4a and b).

Table 3
Mechanical properties of the polymer foams

Sample	Young's modulus [MPa]	Specific Young's modulus [$\text{kPa kg}^{-1} \text{m}^3$]	Crush strength [MPa]	Specific crush strength [$\text{kPa kg}^{-1} \text{m}^3$]
1	5 \pm 1	16 \pm 3	0.3 \pm 0.1	1.0 \pm 0.3
2	25 \pm 5	69 \pm 14	1.6 \pm 0.4	4.4 \pm 1.1
3	26 \pm 4	64 \pm 6	1.8 \pm 0.2	4.4 \pm 0.3
4	69 \pm 4	177 \pm 6	4.9 \pm 0.4	12.6 \pm 0.9
5	99 \pm 6	247 \pm 14	5.1 \pm 0.3	12.8 \pm 0.7
6	120 \pm 10	254 \pm 2	7.3 \pm 0.3	15.4 \pm 0.6

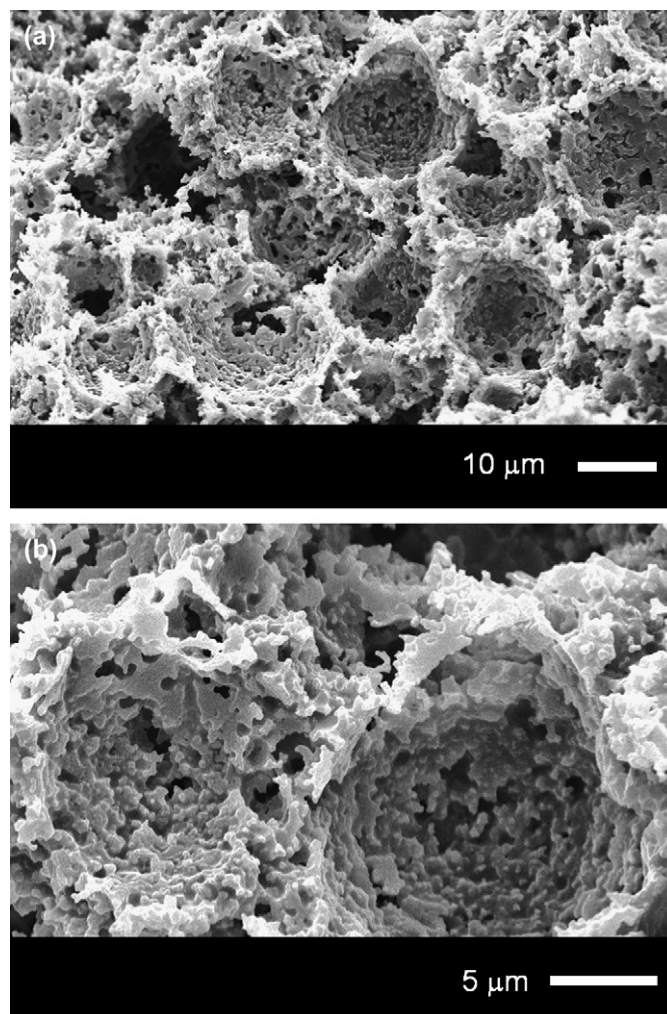


Fig. 2. SEM-micrographs of polyHIPE 1.

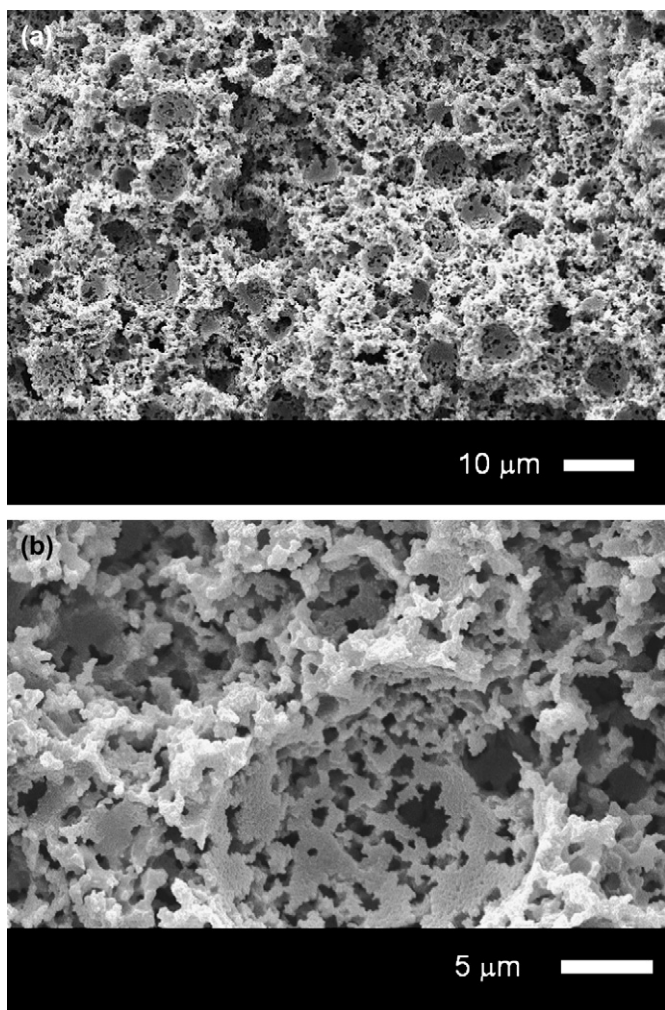


Fig. 3. SEM-micrographs of polyFoam 2.

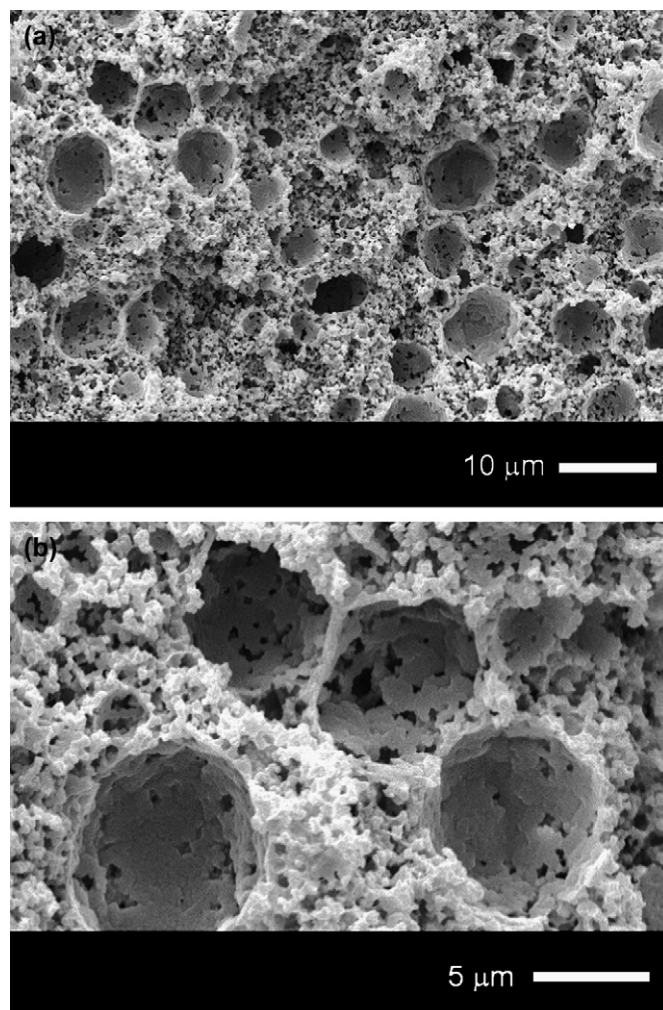


Fig. 4. SEM-micrographs of polyFoam 3.

Nevertheless, polyFoam 3 was a highly porous solid with a matrix density of 1.196 g/cm^3 . The pore diameter ranged from $1 \mu\text{m}$ to $8 \mu\text{m}$ and the pores were interconnected via pore throats of $1 \mu\text{m}$ in diameter. The slight increase in foam density (0.405 g/cm^3) and the decrease in porosity (66%) in comparison to the previously discussed samples were a result of the volume shrinkage during drying (approximately 1%).

MIPEs 4–6 have the same composition as 3 but they also contained up to 30 wt.% silica particles relative to the monomers of the organic phase. PolyFoams 4–6 did not possess the highly open porous structure (Figs. 5–7), which is commonly observed in polyHIPEs (Fig. 2b). The structure was very different from the previously discussed foams. The onset of the formation of the inorganic network formed by the polycondensation of MPS, which is accelerated by the addition of the silica particles, caused these MIPEs to have higher viscosities compared to MIPE 3. Furthermore, the addition of SiO_2 particles to the emulsion and the subsequent vigorous reaction with MPS caused a fast release of methanol, which destabilised the emulsion but also inhibited, at least partially the radical polymerisation. This led to a slight decrease in foam density of the polyFoams 4 (0.389 g/cm^3) and 5 (0.401 g/cm^3) in comparison

to 3 (0.405 g/cm^3) and a drastic change of morphology. The pore diameters of polyFoams 4 and 5 were in the range of $80 \mu\text{m}$ – $120 \mu\text{m}$ (Figs. 5a and 6a). Approximately $20 \mu\text{m}$ thick walls surround the pores (Figs. 5a and 6a). The pore walls had a porous microstructure (Figs. 5b and 6b), which explains the increase in porosity of polyFoams 4 and 5 to 67 and 68%, respectively. The pores were filled with agglomerates of modified silica particles.

MIPE 6 contained 30 wt.% silica particles relative to the monomers in the organic phase. The SEM-micrographs (Fig. 7a) show that the pore size is reduced in comparison to polyFoams 4 and 5 to about $50 \mu\text{m}$. In addition to a microstructure (Fig. 7b), the walls contain small pores of about $10 \mu\text{m}$ in diameter (Fig. 7a and b). These pores are interconnected, but it seems that a thin film covers the pore throats. The silica particles might have helped in this case to stabilise the MIPE, similar to Pickering emulsions [31]. The destabilisation of the emulsion by the formation of methanol causing the emulsion template to collapse, which led to a decrease of the porosity (63%) and an increase of the foam density (0.473 g/cm^3) as compared to 4 and 5. The matrix density of 6 (1.270 g/cm^3) remained unchanged in comparison to 3–5 (Table 2).

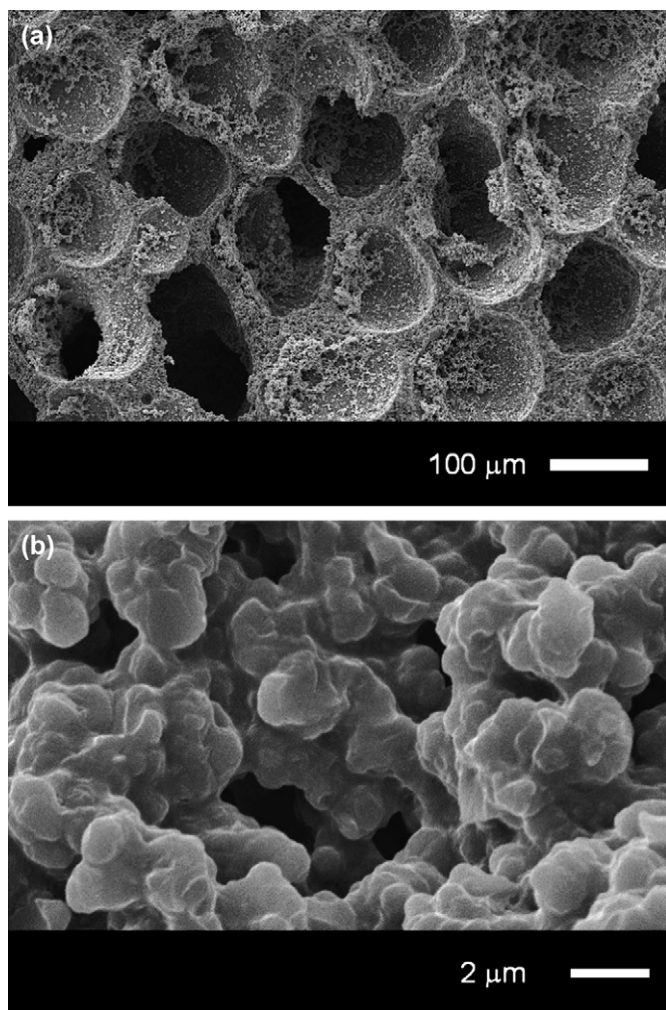


Fig. 5. SEM-micrographs of polyFoam 4.

The mechanical characterisation of all porous polymer monoliths was performed at room temperature under compressive load. Fig. 8 shows representative stress–strain curves for all foams (1–6); the results are summarised in Table 3. The stress–strain behaviour shows an initial elastic region (Fig. 8), the Young's modulus of the samples was determined from its slope. It can be seen that at higher applied stresses the pore structure of all polymer foams collapses if the crush strength is exceeded. The stress–strain curves of 1–3, which did not contain any silica reinforcement, consist of three linear regions with increasing slopes, which is due to the flexibility of the crosslinking agent. The stress–strain curves of the SiO₂ containing polyFoams 4–6, have the typical three regions for polymer foams: the linear elastic, a plateau and the bulk compression region.

Young's modulus of polyHIPE 1 was 5 MPa and the crush strength amounted to 0.3 MPa, which is relatively low in comparison to the other samples but not unusual for polyHIPEs [25]. However, the incorporation of the crosslinker PEGDMA leads to a much increased toughness of the polymer foams as compared to typical polyHIPEs, which are very brittle and chalky. This behaviour is illustrated by three videos, which

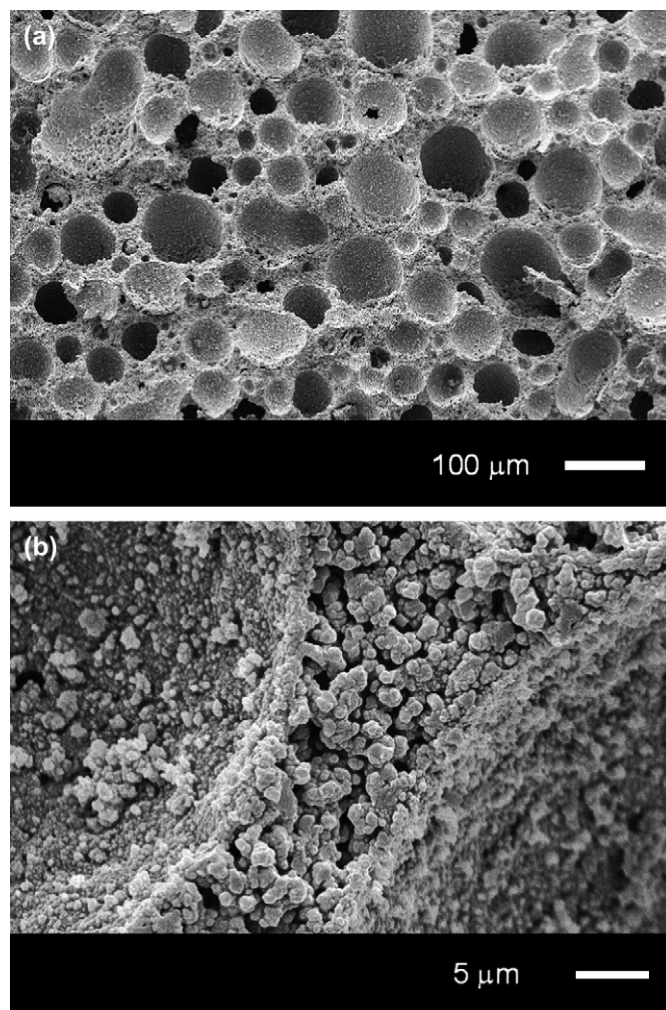


Fig. 6. SEM-micrographs of polyFoam 5.

can be found online.¹ These videos tellingly demonstrate the much-improved toughness of the synthesised polyFoams as compared to conventional DVB-styrene polyHIPEs. The porous polymer monoliths were hit with a 450 g hammer. The conventional polyHIPE is “smashed” into many pieces whereas the polyFoam just rolls to one side. A third video shows the much reduced chalkiness of our polyFoams in direct comparison to a conventional polyHIPE. The chalky character of the polyHIPE, which is due to the low shear resistance of the material, enables to write with the polyHIPE in contrast to the polyFoam. The Young's modulus and the crush strength of polyFoam 2 increased to 25 MPa and 1.6 MPa, respectively, due to the increase in foam density. This was achieved by polymerising the increased continuous organic phase of 40 vol.%. The Young's modulus (26 MPa) and the crush strength (1.8 MPa) of polyFoam 3 were similar to polyFoam 2. The addition of 10 wt.% silica particles to MIPE 4 and their incorporation into the walls of the polymer foam lead to an increase

¹ Please see: A. Menner and A. Bismarck, “Synthesis of porous polymers via emulsion templating”. Link in: <http://www3.imperial.ac.uk/people/a.bismarck/research>; accessed 30.08.06.

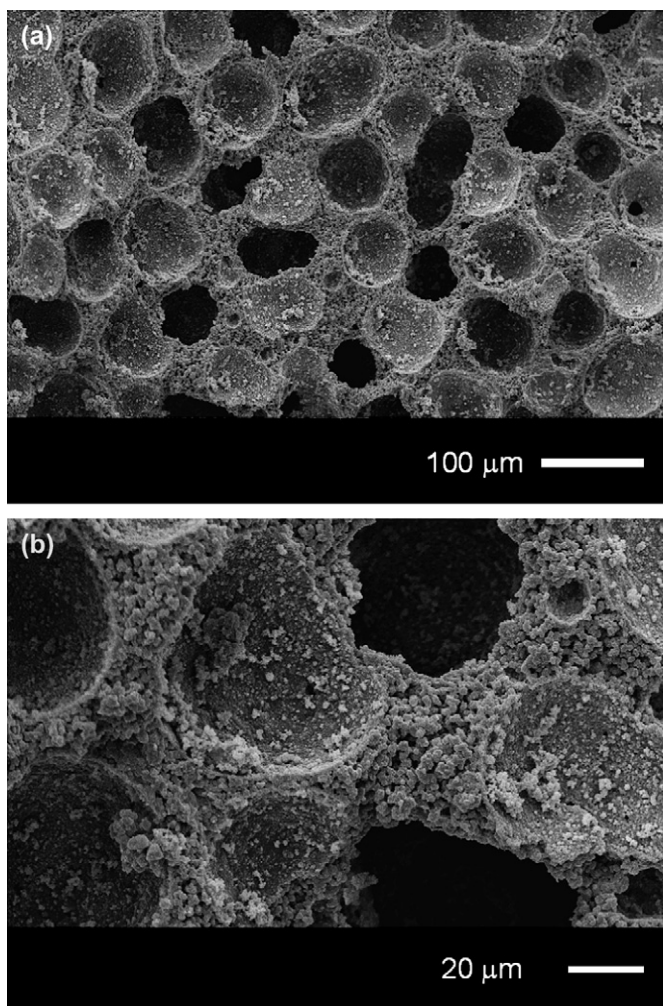


Fig. 7. SEM-micrographs of polyFoam 6.

of Young's modulus and crush strength of polyFoam 4 to 69 MPa and 4.9 MPa, respectively. PolyFoam 5 containing 20 wt.% silica particles had a Young's modulus of 99 MPa and a crush strength of 5.1 MPa. PolyFoam 6 containing

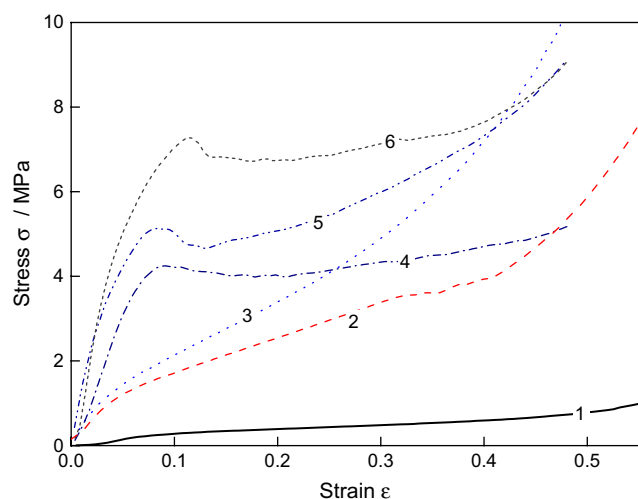


Fig. 8. Exemplar stress–strain curves of the various polymer foam materials under compressive load.

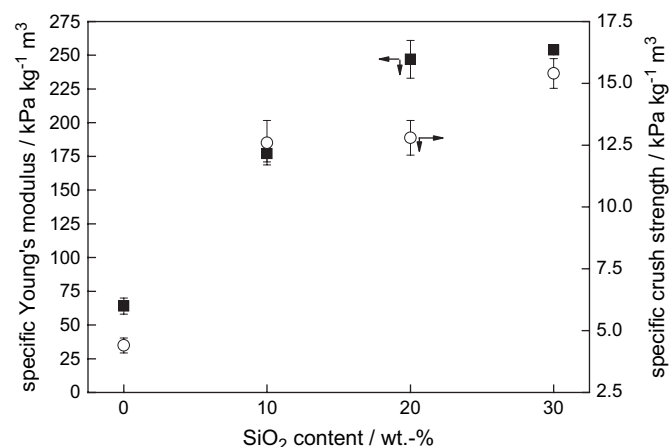


Fig. 9. Specific Young's modulus and specific crush strength of polymer foams synthesised using the same composition but with increasing silica particle loading fraction.

30 wt.% had a Young's modulus of 120 MPa and a crush strength of 7.3 MPa. An increase in the silica particle loading fraction from 10 wt.% to 30 wt.% resulted in a steady increase of specific Young's modulus as well as the specific crush strength for the polyFoams 5 and 6 (Fig. 9). The significant increase of the (specific) Young's modulus as well as (specific) crush strength of silica particle reinforced polyFoams shows that the particles were successfully integrated in the polysil-sesquioxane part of the polymer network by the formation of covalent bonds.

4. Conclusions

The undesired properties, such as brittleness, chalkiness and the overall poor mechanical performance of conventional polyHIPEs, have so far hindered many major applications. Our main objective was to enhance the mechanical properties of very porous polymer foams possessing an interconnected pore network structure. We successfully integrated a stress-reducing component, PEGDMA, as a crosslinker into the polymer network forming the foam. This resulted in much reduced brittleness and chalkiness of the synthesised polymer foams. We adapted two more strategies to improve the mechanical performance of polymer foams prepared from concentrated emulsion templates: firstly, we increased the organic phase volume from 20 to 40% to increase the monomer concentration which results in porous polymer monolith with much increased foam densities. Secondly, we added silica particles to the emulsion to reinforce the inorganic component formed by the hydrolysis of MPS of the polymer network forming the polyFoams.

The polyFoams 2–6 were prepared by the polymerisation of the continuous phase of concentrated emulsions containing 40 vol.% organic phase. The nonionic polymeric surfactant Hypermer B246sf was well suited to stabilise such emulsions. The resulting polyFoams were highly porous and possessed the characteristic interconnected pore structure for polyHIPEs. The increase of the organic phase level resulted in an

increased foam density, which led to much-improved overall mechanical performance as compared to the “traditional” polyHIPEs.¹

The addition of reinforcement to the liquid formulation did not inversely affect the stability of the concentrated emulsion; however, upon polymerisation the polyFoams did not possess the characteristic open porous network structure. Nevertheless, the walls surrounding the bigger pores of the foams were highly porous. The silica particles have been successfully integrated into the polymer matrix of polymer foams. The particles acted as reinforcement of the inorganic polysilsesquioxane component of the polymer network, which led to a significant increase of Young’s modulus as well as crush strength in comparison to samples that did not contain any reinforcement; Young’s modulus of polyFoam **5** increased by 280% and that of polyFoam **6** by 361% compared to the polyFoam **3** containing no filler. The crush strength of the reinforced samples increased by up to 303% in comparison to the non-reinforced sample **3**.

Acknowledgements

The authors would like to thank Halliburton Energy Services for funding this research. AM was a Halliburton visiting research fellow.

References

- [1] Lissant KJ. *J Soc Cosmet Chem* 1970;21:141–54.
- [2] Mezzenga R, Ruokolainen J, Fredrickson GH. *Macromolecules* 2003; 36:4466–71.
- [3] Tai H, Sergienko A, Silverstein MS. *Polym Eng Sci* 2001;41:1540–52.
- [4] Sergienko A, Tai H, Narkis M, Silverstein M. *J Appl Polym Sci* 2002;84:2018–27.
- [5] Cameron NR, Sherrington DC. *J Mater Chem* 1997;7:2209–12.
- [6] Cameron NR, Sherrington DC, Ando I, Kurosu H. *J Mater Chem* 1996;6:719–26.
- [7] Cameron NR, Barbetta A. *J Mater Chem* 2000;10:2466–72.
- [8] Menner A, Bismarck A. *Macromol Symp*, in press.
- [9] Williams JM, Gray AJ, Wilkerson MH. *Langmuir* 1989;6:437–44.
- [10] Lissant KJ, Mayhan KG. *J Colloid Interface Sci* 1973;42:201–8.
- [11] Barby D, Haq Z. *European Patent* 60 138; 1982.
- [12] Barby D, Haq Z. *United States Patent* 4522953; 1985.
- [13] Haq Z. *European Patent* 105634; 1984.
- [14] Akay G. *European Patent* 1526914; 2005.
- [15] Halisington MA, Duke JR, Apen PG. *Polymer* 1997;38:3347–57.
- [16] Choi JS, Chun BC, Lee SJ. *Macromol Res* 2003;11:104–9.
- [17] Wakeman RJ, Bhungara ZG, Akay G. *Chem Eng J* 1998;70:133–41.
- [18] Krajnc P, Stefanec D, Brown JF, Cameron NR. *J Polym Sci Part A Polym Chem* 2005;43:296–303.
- [19] Bokhari MA, Akay G, Zhang SG, Birch MA. *Biomaterials* 2005;26: 5198–208.
- [20] Hayman MW, Smith KH, Cameron NR, Przyborski SA. *Biochem Biophys Res Commun* 2004;314:483–8.
- [21] Hayman MW, Smith KH, Cameron NR, Przyborski SA. *J Biochem Biophys Methods* 2005;62:231–40.
- [22] Jones K, Lothian BR, Martin A, Taylor G, Haq Z. *European Patent* 156541; 1985.
- [23] Krajnc P, Brown JF, Cameron NR. *Org Lett* 2002;4:2497–500.
- [24] Sergienko AY, Tai HW, Narkis M, Silverstein MS. *J Appl Polym Sci* 2004;94:2233–9.
- [25] Tai H, Sergienko A, Silverstein MS. *Polymer* 2001;42:4473–82.
- [26] Colin A, Carn F, Achard M-F, Birot M, Deleuze H, Backov R. *J Mater Chem* 2004;14:1370–6.
- [27] Lissant KJ. *J Colloid Interface Sci* 1966;22:462–8.
- [28] Menner A, Powell R, Bismarck A. *Macromolecules* 2006;39:2034–5.
- [29] Menner A, Powell R, Bismarck A. *Soft Matter* 2006;2:337–42.
- [30] Haibach K, Menner A, Powell R, Bismarck A. *Polymer* 2006;47: 4513–9.
- [31] Binks BP, Clint JH. *Langmuir* 2002;18:1270–3.